Bioorganic & Medicinal Chemistry Letters 25 (2015) 2679–2685

Contents lists available at ScienceDirect

Bioorganic & Medicinal Chemistry Letters

journal homepage: www.elsevier.com/locate/bmcl

Design of selective PI3Kα inhibitors starting from a promiscuous pan kinase scaffold

Bernard Barlaam [a,*], Sabina Cosulich [a], Martina Fitzek [a], Stephen Green [a], Craig S. Harris [b,†], Kevin Hudson [a], Christine Lambert-van der Brempt [b], Gilles Ouvry [b,†], Ken Page [a], Linette Ruston [a], Lara Ward [a], Bénédicte Delouvrié [b,*]

[a] AstraZeneca, Oncology iMed, Alderley Park, Macclesfield, Cheshire SK10 4TG, United Kingdom
[b] AstraZeneca, Centre de Recherches, Z.I. La Pompelle, B.P. 1050, Chemin de Vrilly, 51689 Reims Cedex 2, France

ARTICLE INFO

Article history:
Received 4 March 2015
Revised 20 April 2015
Accepted 22 April 2015
Available online 29 April 2015

Keywords:
PI3Kα inhibitor
Kinase selectivity

ABSTRACT

Starting from compound **1**, a potent PI3Kα inhibitor having poor general kinase selectivity, we used structural data and modelling to identify key exploitable differences between PI3Kα and the other kinases. This approach led us to design chemical modifications of the central pyrazole, which solved the poor kinase selectivity seen as a strong liability for the initial compound **1**. Amongst the modifications explored, a 1,3,4-triazole ring (as in compound **4**) as a replacement of the initial pyrazole provided good potency against PI3Kα, with excellent kinase selectivity.

Signalling pathways mediated by the phosphatidylinositol 3-kinase (PI3K) family play a central role in a number of cell processes including proliferation and survival. Deregulation of these pathways is a causative factor of a wide spectrum of human cancers and other diseases.[1] The most studied and understood class of these lipid kinases is the Class I PI3K, which is sub-divided into Class Ia and Class Ib enzymes on the basis of their regulatory partners and mechanism of regulation.[2] Class Ia enzymes consist of three distinct catalytic subunits (p110α, p110β and p110δ, respectively, for the PI3Kα,β and δ isoforms) which dimerise with regulatory subunits (such as p85α). Class Ia PI3K enzymes are generally activated in response to growth factor stimulation of receptor tyrosine kinases, via interaction of the regulatory subunit SH2 domains with specific phospho-tyrosine residues of the activated receptor or adaptor proteins. Both p110α and p110β are widely expressed across cell types and tissues, whereas p110δ expression is more restricted to leucocyte populations and some epithelial cells. Achieving selectivity for PI3Kα versus PI3Kβ might therefore improve tolerability when compared with pan-PI3K inhibitors.

There is now considerable evidence indicating that Class Ia PI3K enzymes contribute to tumourigenesis in a wide variety of human cancers, either directly or indirectly.[3] In particular, the PIK3CA gene, which encodes the p110α catalytic subunit of PI3Kα, is widely implicated in tumourigenesis. Activating point mutations, found predominantly in the helical or catalytic domains of p110α, increase the PI3K kinase activity of the holoenzyme and can transform cells. These activating mutations occur at significant frequencies across a wide range of tumour types, particularly as somatically occurring mutations.[4] Tumour-related mutations in p85α have also been identified in cancers such as those of the ovary and colon.[5] Furthermore, the p110α subunit is amplified in some tumours such as those of the ovary[6] and cervix.[7]

Early studies, both pre-clinical and clinical, exploring the physiological and pathological roles of the PI3K enzymes, have largely used agents with limited kinase selectivity, either encompassing diverse kinase families, or restricted to the PI3K related kinase (PIKK) family, or selective for the PI3K Class I family. These have demonstrated limited clinical utility to date, often limited by their toxicity.[8] Hence, there is a need for more isoform-selective PI3K inhibitors to provide useful therapeutic agents with the potential to deliver an improved therapeutic margin over these initial clinical agents.[9]

In this Letter, starting from a fairly promiscuous pan kinase early lead compound, we report the identification of inhibitors that are both selective for the PI3Kα over the PI3Kβ isoform and with a much improved general kinase selectivity. Selectivity among the PI3K isoforms was routinely measured with enzyme assays and the α/β selectivity was also monitored in cell assays (inhibition of AKT phosphorylation at Thr308 in human breast ductal carcinoma BT474 cells, that contain a PIK3CA gene mutation increasing their dependency on PI3Kα, and at Ser473 in breast

* Corresponding authors.
E-mail address: bernard.barlaam2@astrazeneca.com (B. Barlaam).
† Current address: Galderma R&D, les Templiers, 2400 route des Colles, 06410 Sophia-Antipolis, France.

http://dx.doi.org/10.1016/j.bmcl.2015.04.084
0960-894X/

adenocarcinoma MDA-MB-468 cells, that have lost the PTEN gene increasing their dependency on PI3Kβ, providing measurements of PI3Kα and PI3Kβ inhibition, respectively).[10] Kinase promiscuity was routinely measured using several kinase enzyme assays against VEGF-R2 (KDR), Aurora B, FGFR1, GSK3β, but since potency for all of these kinases correlated with KDR then, for simplicity, only the KDR enzyme results are reported in this Letter.

Our primary goal was to develop a PI3K inhibitor selective for PI3Kα versus PI3Kβ. During the lead generation effort of this project, we identified a benzotriazole aminopyrazine series showing some degree of selectivity for PI3Kα versus PI3Kβ, exemplified by compound **1** (Fig. 1). However, this compound had activity against additional kinases (13 additional kinases with >80% inhibition at 1 μM out of 76 kinases in the 'Dundee University protein kinase' panel, see Fig. 3) and this lack of selectivity was confirmed in our internal kinase assays. We anticipated that the identity of some of those anti-targets (e.g., KDR, Aurora B, FGFR1, GSK3β) and their known pharmacological effects might lead to an unacceptable safety profile. Therefore it was considered mandatory to remove the pan-kinase inhibition liability if this chemical series was to progress further.

Detailed structural analysis and docking were carried out in order to identify key exploitable differences between PI3Kα and the anti-targets we did not want to inhibit. Docking of compound **1** in the publicly available crystal structure[11] of PI3Kα (Fig. 2a) was performed manually, on the basis of the binding mode of aminopyrazine derivatives observed in several in-house kinase crystal structures (unpublished results). Further refinement of the model was carried out, taking into account the particular environment of the PI3Kα ATP binding site and the SAR data available in our series. In particular, we considered that the sp^2 nitrogen of the pyrazole ring in compound **1** (labelled N^3 thereafter) plays a key role in PI3Kα potency, but also in α/β selectivity. Indeed, in our model, it is located at an H-bond distance from the Gln859 residue, which is unique to the PI3Kα isoform. The equivalent residue in PI3Kβ is an aspartic acid (Asp861), which is unsuitable to interact favourably with N^3. During the course of this work, another group reported that hydrogen bond interactions with the Gln859 side chain is the structural determinant for PI3Kα selectivity in their aminothiazole series, leading to the identification of NVP-BYL719, a selective PI3Kα inhibitor.[12]

Similar docking of compound **1** was performed in a few anti-targets whose experimental 3D structure was available. In

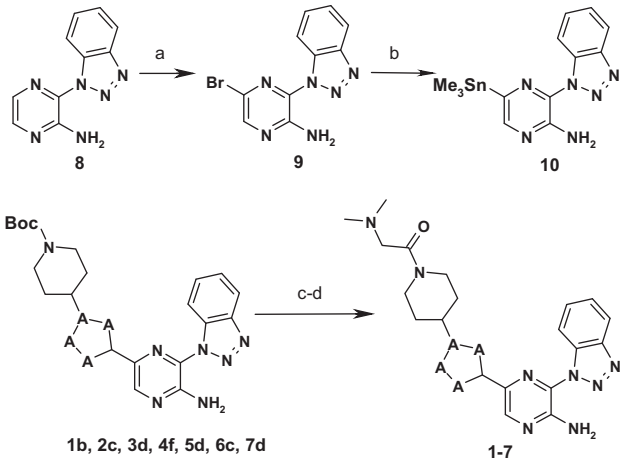

Scheme 1. General synthesis of compounds **1**–**7**. Reagents and conditions: (a) 1-bromopyrrolidine-2,5-dione, DMF, 40 °C, 1 h, 72%; (b) $(PPh_3)_4Pd$, $(Me_3Sn)_2$, toluene, 110 °C, 2 h, 54%; (c) HCl, isopropanol, 75 °C, 2 h or TFA, rt, 1 h, 62–98%; (d) NEt_3, $Me_2NCH_2C(=O)Cl$, DMF or CH_2Cl_2, rt, 2 h or NEt_3, $Me_2NCH_2CO_2H$, TBTU, CH_2Cl_2, rt, overnight, 47–91%.

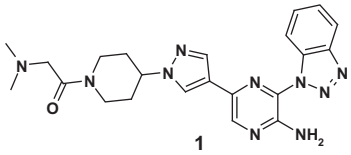

PI3Kα enz IC_{50} : 0.016 μM
PI3Kβ enz IC_{50} : 0.9 μM
KDR enz IC_{50} : 0.029 μM
PI3Kα cell IC_{50} : 0.058 μM
PI3Kβ cell IC_{50} : 13 μM

Figure 1. Structure of compound **1** and its biological activity against PI3K and KDR enzymes.

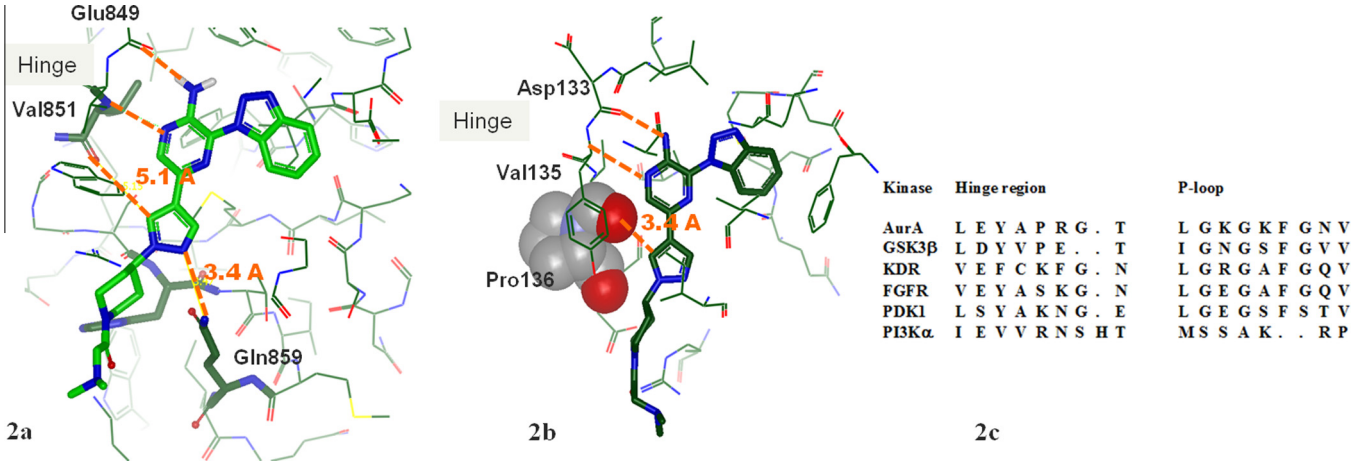

Figure 2. (a) Docking of **1** in PI3Kα. Protein residues are in green sticks representation, compound **1** in green capped sticks. The aminopyrazine moiety binds to the hinge region through an H-bond donor/acceptor network (orange dotted lines). A putative H-bond between the pyrazole N^3 and the unique Gln859 residue is illustrated. (b) Docking of **1** in GSK3β, based on previous structures of aminopyrazines in GSK3β.[13] The two backbone carbonyl groups pointing towards the binding site are highlighted in van der Waals spheres. The distance between one of the backbone carbonyl and the closest pyrazole carbon is significantly shorter than in PI3Kα. (c) Sequence alignment of a few representative anti-target kinases with PI3Kα, focused on the hinge and P loop regions.

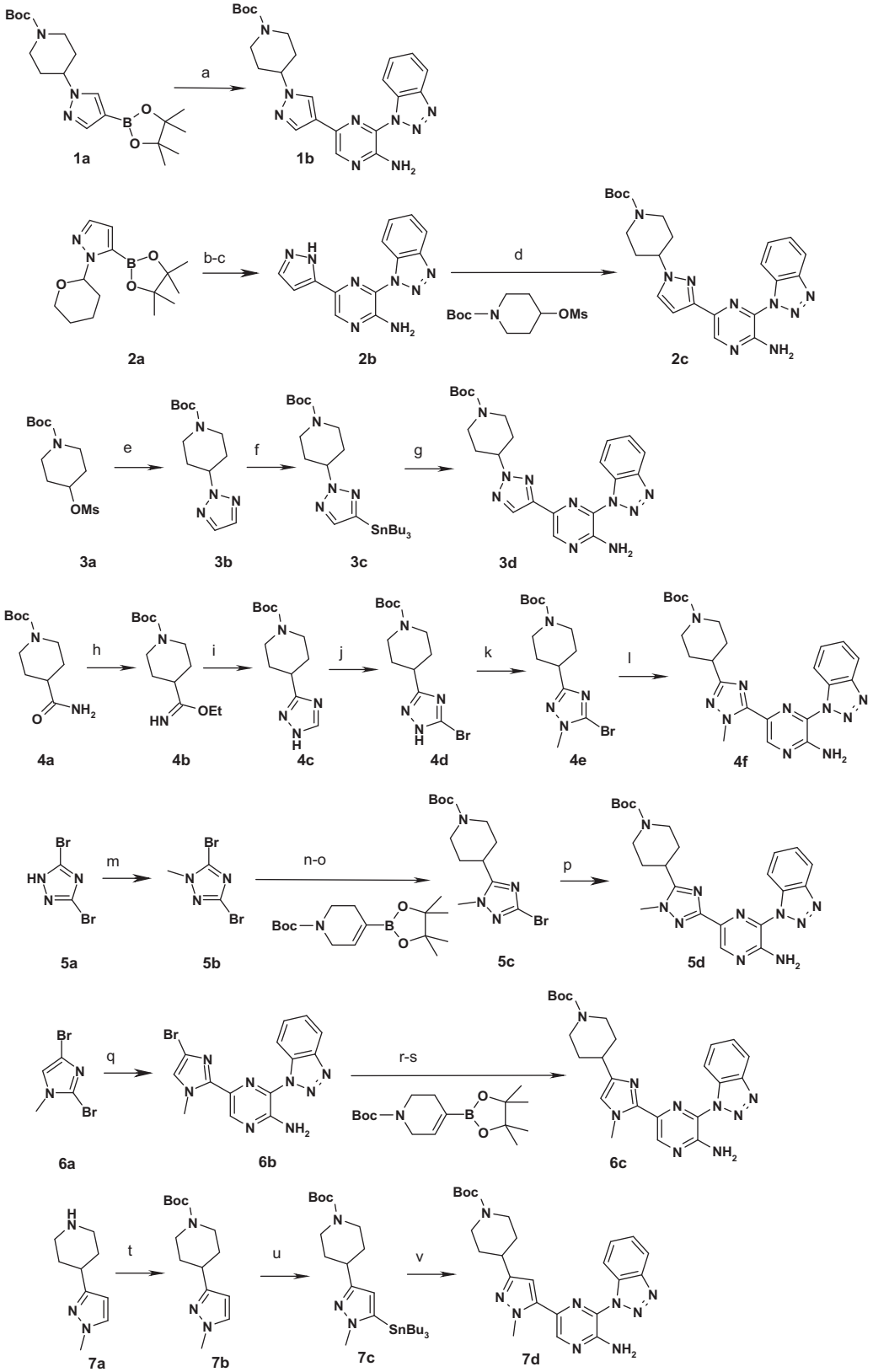

Scheme 2. Detailed synthesis of each five-membered heteroaryl. (a) **9**, $(PPh_3)_2PdCl_2$, CsF, isopropanol, reflux, 4 h, 82%; (b) **9**, $(PPh_3)_2PdCl_2$, CsF, methanol, 140 °C, microwave, 45 min, 63%; (c) HCl, isopropanol, 75 °C, 1 h, 94%; (d) tripotassium phosphate, DMA, 80 °C, 2 days, 38%; (e) 1,2,3-triazole, NaH, DMF, 60 °C, 5 days, 29%; (f) BuLi, THF, −78 °C then Bu_3SnCl, 70%; (g) **9**, $(PPh_3)_2PdCl_2$, LiCl, DME, 150 °C, 0.5 h, 31%; (h) triethyloxonium hexafluorophosphate, CH_2Cl_2, rt, overnight, 95%; (i) formohydrazide, dioxane, 40–80 °C overnight, 86%; (j) NaOH then benzyltrimethylammonium tribromide, CH_2Cl_2, 79%; (k) diazomethyltrimethylsilane, toluene/methanol, rt, 47%; (l) **10**, $(PPh_3)_2PdCl_2$, LiCl, 4-methyl-2-pentanol, 130 °C, 5 h, 91%; (m) NaH, DMF then MeI, rt, overnight, 83%; (n) $(PPh_3)_2PdCl_2$, CsF, methanol, 110 °C, microwave, 25 min, 73%; (o) PtO_2, ethanol, rt, 3 h, 51%; (p) **10**, $(PPh_3)_2PdCl_2$, LiCl, DME, 140 °C, microwave, 60 min, 71%; (q) **10**, $(PPh_3)_2PdCl_2$, LiCl, methanol, 130 °C, microwave, 35 min, 61%; (r) $(PPh_3)_2PdCl_2$, CsF, methanol, 130 °C, microwave, 40 min, 64%; (s) Pd, formic acid, DMF, 70 °C, 2 h, 63%; (t) $(Boc)_2O$, NEt_3, CH_2Cl_2, 0–25 °C, 85%; (u) LDA, $Me_2CH_2CH_2NMe_2$, then Bu_3SnCl, −70 to 0 °C, THF, 43%; (v) **9**, $(PPh_3)_2PdCl_2$, LiCl, DME, 150 °C, 0.5 h, 65%.

Table 1
Properties of compounds **1**–**7**

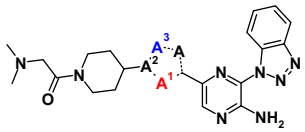

Compound	Ring	PI3Kα enz IC_{50}[a]	PI3Kβ enz IC_{50}[a]	KDR enz IC_{50}[a]	PI3Kα cell IC_{50}[a]	PI3Kβ cell IC_{50}[a]	Log $D_{7.4}$	pK_β N^1	pK_β N^3
1	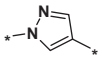	0.016	0.9	0.029	0.058	13	1.7	–	2.2
2	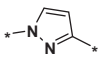	0.027	1.7	0.17[b]	0.25	10	1.8	1.6	–
3	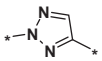	0.021	0.65	0.21	0.14	7.8	1.9	0.8	1.4
4	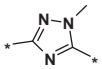	0.029	1.0	9.0	0.27	6.9	0.9	2.2	1.9
5	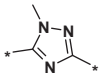	0.28	2.4	1.2[b]	3.9[b]	12[b]	1.0	2.1	–
6	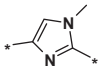	0.064	1.3	6.6[b]	0.69	7.9	1.3	2.7	–
7	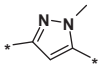	0.006	0.38	0.09	0.091	4.3	1.8	–	2.5

[a] μM; unless stated otherwise, numbers are a geometric mean of 2 or more values.
[b] $n = 1$ value.

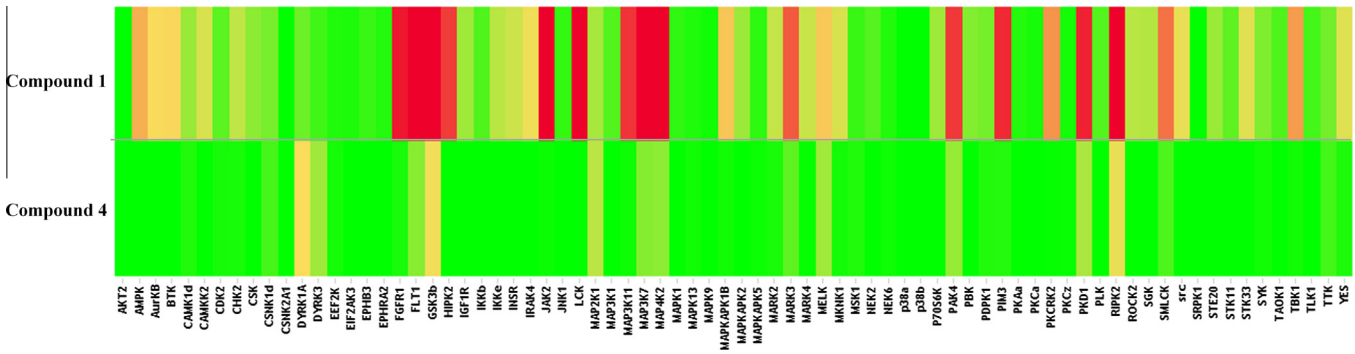

Figure 3. Heat map showing the inhibitory activity of compounds **1** and **4** against a panel of 76 kinases ('Dundee University protein kinase' panel) at 1 μM. The percentage of inhibition is coloured from green (0%) to yellow (60%) and red (90%).

particular, docking of **1** in the publicly available crystal structures[13] of GSK3β highlighted useful differences (Fig. 2b), including two regions that might be exploited to gain selectivity.

Firstly, the hinge region: most of the anti-targets have a shorter hinge sequence and some have two backbone carbonyls facing the pyrazole ring of **1** (highlighted with red balls in Fig. 2b). This is exemplified in GSK3β which bears a proline residue in this region (Fig. 2c). By contrast, in PI3Kα there is only one carbonyl pointing towards the pyrazole and at a longer distance than that observed in GSK3β (Fig. 2a and b). One of the ideas considered was the introduction of a nitrogen atom on the pyrazole ring to create an electronic repulsion with the two carbonyls in the anti-targets.

Secondly, the backpocket also shows some differences with a longer P loop carrying more lipophilic hindered residues in the anti-targets (Fig. 2c). Another idea considered was adding substituents on the benzotriazole moiety in order to create steric clashes with the anti-targets.

From the different ideas we explored, we did not see any benefit regarding kinase selectivity with the different substituted benzotriazoles. However, replacing the pyrazole ring was advantageous and is the main focus of this Letter. During our work modifying the pyrazole ring, we assessed the hypothesis of the key role played by the N^3 nitrogen, in particular replacing the N^3 nitrogen with a CH in some examples as a confirmation of our docking hypothesis.

Compounds **1**–**7** were made according to Schemes 1 and 2.[14] Syntheses were unique to each five-membered heteroaryl, but all syntheses used the common aminopyrazine intermediates **9** or **10**. Bromide **9** was made from the previously described synthon **8**[15] and the stannane **10** was made from **9** by palladium catalysed stannylation. All syntheses also had a Boc protected piperidine and shared the same last two steps: Boc group was removed under acidic conditions (TFA or HCl) and then the piperidine amide was installed via an amide coupling from the carboxylic acid or by

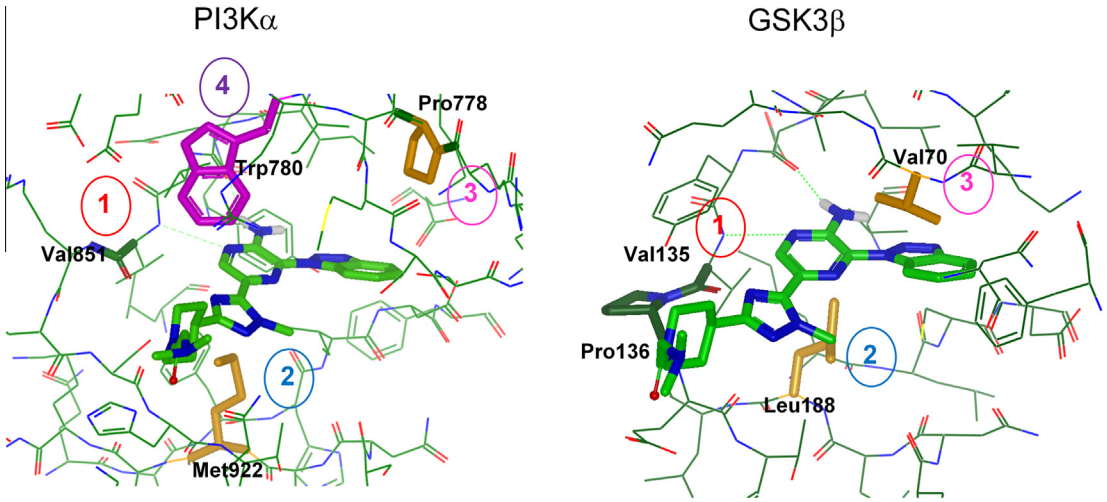

Figure 4. Docking of compound **4** in PI3Kα (left) and GSK3β (right). The different areas highlighted illustrate hypotheses for the PI3Kα selectivity of **4** versus other kinases.

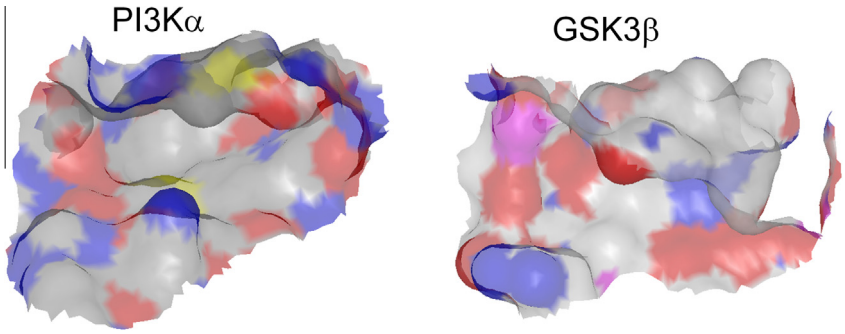

Figure 5. Molecular surface of PI3Kα and GSK3β inhibitor binding site coloured by hydrogen bond potential (red: strong acceptor; blue: strong donor; magenta: OH group; yellow: sulfur; grey: lipophilic).

acylation with the acid chloride analogue to yield compounds **1**–**7** in good yields.

The Boc piperidines **1b**, **2c**, **3d**, **4f**, **5d**, **6c** and **7d** were prepared according to Scheme 2. We trialed numerous strategies which, for the most part, are interchangeable. It should be noted that, although quite a few reactions in this scheme produced mixtures of regioisomers, all regioisomers were separated by standard chromatographic techniques. The desired regioisomer was always the major compound formed and, for clarity, it is the only one reported on the scheme. Whereas the 1,4-disubstituted pyrazole **1b** was accessible by a *Suzuki–Miyaura* cross coupling from the known boronic ester **1a**,[16] little precedent existed for the other rings in the literature. Routes to these rings are described below. The 1,3-disubstituted pyrazole **2b** was also prepared by *Suzuki–Miyaura* coupling but the piperidine was installed after via a mesylate displacement to provide **2c** in acceptable yield. Our first attempts at preparing the boronic acid pinacol esters (Bpin) of 1,2,3- and 1,3,4-triazoles were not conclusive for stability or reactivity reasons.[17] Consequently, we were forced to adopt the environmentally less friendly *Stille* coupling using the stable stannanes **3c** and **10**. Starting from mesylate **3a**, displacement by 1,2,3-triazole under basic conditions followed by a stannylation gave **3c**, which coupled well with bromide **9** to deliver **3d**. The 1,3,4-triazole example **4** was the only ring to be formed by cyclisation due to issues in preparing a C-5 boronic acid or stannane derivative for which there are very few references.[18] The primary amide **4a** was transformed to imidate **4b**[19] and cyclised to **4c** with formohydrazide. A bromination–methylation sequence gave the major regioisomer **4e**, which was coupled with stannane **10** to form **4f**. Regioisomer **5** could have been delivered as a secondary product of this sequence. However another sequence from symmetrical di-bromotriazole reagent **5a** was preferred. Methylation of **5a** and *Suzuki–Miyaura* coupling, followed by reduction of the double bond using platinum on carbon, provided the side chain regio-isomer **5c**. *Stille* coupling with stannane **10** finally afforded **5d**. To access **6c**, we carried out the regioselective *Stille* coupling of 3,5-dibromo-1-methylimidazole **6a** to afford **6b** in good yield.[20] The subsequent *Suzuki–Miyaura* coupling worked well. However, hydrogenation of the piperidine double bond routinely required a stoichiometric quantity of palladium on charcoal to give **6c**, presumably due to catalyst poisoning by the aminopyrazine fragment. Finally, Boc protection from commercially available **7a** afforded **7b**, which, after deprotonation, was converted to the stannane **7c**. Coupling with **9** afforded **7d** in good yield.

A first encouraging result was observed with the pyrazole isomer compound **2** and the 1,2,3-triazole compound **3** (Table 1). Both rings maintained potency against PI3Kα but lost 10-fold potency against KDR compared to compound **1**. However, more than another order of magnitude increase in selectivity was achieved with the 1,2,4-triazole analogue **4**, with an IC_{50} of only 9 μM against KDR. A significant reduction of $\log D_{7.4}$ was measured for this ring. The position of the methyl was critical to maintain potency against PI3Kα, as shown by the 10-fold decrease of PI3Kα enzyme potency between compounds **4** and **5**. Indeed, in our docking model, the methyl in compound **5** clashed with Gln859 in PI3Kα. Imidazole **6** also lost some potency against

PI3Kα compared to **4**, as a consequence of replacing N^3 by a CH. Interestingly, **6** was poorly active against KDR. Pyrazole **7** confirmed the importance of N^3 for good potency against PI3Kα, but the selectivity versus KDR was lost as a consequence of not having a nitrogen atom at A^1. The PI3Kα cell data confirmed the PI3Kα potency ranking seen at the enzyme level for compounds **1**–**7**.

Looking at N^1, N^3 and $\log D_{7.4}$ separately, it was not straightforward to fully rationalise the results. In particular, the difference of activity against KDR between the two triazole isomers **3** and **4** was not anticipated to be so significant. In order to assess our initial hypothesis, pK_β values were calculated for N^1 and N^3 when present in the molecules.[21] A pK_β value represents the ability of a heteroatom (H-bond acceptor) to form a hydrogen bond with an H-bond donor (X-H). We noticed that the pK_β of N^1 was inversely correlated with KDR potency (the higher the pK_β, the better the selectivity), whilst the pK_β of N^3 was somewhat correlated to PI3Kα potency. A N^1 pK_β greater than 2 appeared necessary in order to reduce activity against KDR to a micromolar level. This might be why triazoles **3** and **4** had such different potency against KDR. On the other hand, if N^3 pK_β was high, interaction with Gln859 would be strong and potency against PI3Kα might increase. With this hypothesis in mind, we compared the imidazole **6** and the pyrazole **7**. **7**, having the strongest N^3 pK_β, was the most active on PI3Kα, but did not show selectivity versus KDR, due to the absence of any strong H-bond acceptor at A^1. On the other hand, **6**, having the strongest N^1 pK_β, displayed excellent selectivity versus KDR (similar to **4**) but only modest potency against PI3Kα, due to the absence of any strong H-bond acceptor at A^3.

More rings were explored during our programme but none afforded a better kinase selectivity and potency against PI3Kα than the 1,2,4-triazole exemplified by compound **4**. The significant progress achieved in kinase selectivity between pyrazole **1** and triazole **4** is pictured in the kinase heatmap, Figure 3. Whilst **1** had 13 undesired kinase hits with >80% inhibition at 1 μM, **4** only hits moderately (~60%) 3 kinases: RIPK2, DYRK1A and GSK3β.[22]

While the goal of adding a nitrogen to the pyrazole ring was to induce an electronic repulsion with the anti-targets (area 1 on Fig. 4), we cannot discount the additional impact of other structural factors on kinase selectivity. In particular the methyl group on the 1,3,4-triazole in compound **4** may have an unfavouring effect on KDR, because the flexible methionine (Met922) in PI3Kα is replaced with a highly conserved more rigid leucine in the anti-targets, Leu188 for GSK3β (area 2 on Fig. 4). Moreover, a conformational analysis showed that this same methyl forces the benzotriazole moiety to twist by 30°, which may induce a clash with a conserved valine (Val70 for GSK3β) in the P loop of the anti-targets, whereas such a negative interaction is unlikely with the more distant proline (Pro778) in PI3KPI3Kα (area 3). Another noticeable difference between the PI3Ks and the protein kinase family is the presence of a tryptophan residue (Trp780) in the upper lobe of the ATP binding site. This tryptophane might help the triazole to fit into PI3Kα by 'closing' the upper loop with a strong face to edge interaction, absent in the anti-targets (area 4). Finally the polarity of the inhibitor binding site varies from one kinase to another. The more hydrophilic 1,3,4-triazole may be better tolerated in PI3Kα than in the less polar anti-targets binding cavity (Fig. 5).

In conclusion, starting from compound **1**, a potent PI3Kα inhibitor having poor general kinase selectivity, we used structural data and modelling to identify key exploitable differences between PI3Kα and the anti-targets. Chemical modifications of the central pyrazole improved dramatically the kinase selectivity that was seen as a significant liability for the initial compound **1**. In particular, a 1,3,4-triazole ring (as in compound **4**) as a replacement of the initial pyrazole provided good potency against PI3Kα, with excellent kinase selectivity. Further optimisation of compound **4** will be reported in due course.

Acknowledgments

We acknowledge the following scientists for their contribution in the synthesis or characterization of the compounds: Christian Delvare, Delphine Dorison Duval, Hervé Germain, Maryannick Lamorlette, Françoise Magnien, and the members of the SAR Screening Groups for generating the cell and biochemical data.

References and notes

1. (a) Katso, R.; Okkenhaug, K.; Ahmadi, K.; White, S.; Timms, J.; Waterfield, M. D. *Dev. Biol.* **2001**, *17*, 615; (b) Foster, F. M.; Traer, C. J.; Abraham, S. M.; Fry, M. J. *J. Cell Sci.* **2003**, *116*, 3037.
2. Engelman, J. A.; Luo, J.; Cantley, L. C. *Nat. Rev. Genet.* **2006**, *7*, 606.
3. Vivanco, I.; Sawyers, C. L. *Nat. Rev. Cancer* **2002**, *2*, 489.
4. (a) Samuels, Y.; Wang, Z.; Bardelli, A.; Silliman, N.; Ptak, J.; Szabo, S.; Yan, H.; Gazdar, A.; Powell, S. M.; Riggins, G. J.; Willson, J. K.; Markowitz, S.; Kinzler, K. W.; Vogelstein, B.; Velculescu, V. E. *Science* **2004**, *304*, 554; (b) Samuels, Y.; Diaz, L. A., Jr.; Schmidt-Kittler, O.; Cummins, J. M.; Delong, L.; Cheong, I.; Rago, C.; Huso, D. L.; Lengauer, C.; Kinzler, K. W.; Vogelstein, B.; Velculescu, V. E. *Cancer Cell.* **2005**, *7*, 561.
5. Philp, A. J.; Campbell, I. G.; Leet, C.; Vincan, E.; Rockman, S. P.; Whitehead, R. H.; Thomas, R. J.; Phillips, W. A. *Cancer Res.* **2001**, *61*, 7426.
6. Shayesteh, L.; Lu, Y.; Kuo, W. L.; Baldocchi, R.; Godfrey, T.; Collins, C.; Pinkel, D.; Powell, B.; Mills, G. B.; Gray, J. W. *Nat. Genet.* **1999**, *1*, 99.
7. Ma, Y. Y.; Wei, S. J.; Lin, Y. C.; Lung, J. C.; Chang, T. C.; Whang-Peng, J.; Liu, J. M.; Yang, D. M.; Yang, W. K.; Shen, C. Y. *Oncogene* **2000**, *19*, 2739.
8. Fruman, D. A.; Rommel, C. *Nat. Rev. Drug Disc.* **2014**, *13*, 140.
9. Thorpe, L. M.; Yuzugullu, H.; Zhao, J. J. *Nat. Rev. Cancer* **2015**, *15*, 7.
10. Barlaam, B.; Cosulich, S.; Degorce, S.; Fitzek, M.; Green, S.; Hancox, U.; Lambert-van der Brempt, C.; Lohmann, J.-J.; Maudet, M.; Morgentin, R.; Pasquet, M.-J.; Péru, A.; Plé, P.; Saleh, T.; Vautier, M.; Walker, M.; Ward, L.; Warin, N. *J. Med. Chem.* **2015**, *58*, 943.
11. Mandelker, D.; Gabelli, S. B.; Schmidt-Kittler, O.; Zhu, J.; Cheong, I.; Huang, C. H.; Kinzler, K. W.; Vogelstein, B.; Amzel, L. M. *Proc. Natl. Acad. Sci. U.S.A.* **2009**, *106*, 16996. The crystal structure of PI3Kα in complex with Wortmannin was used to dock compounds **1** and **4** (PDB ID code: 3hhm).
12. Furet, P.; Guagnano, V.; Fairhurst, R. A.; Imbach-Weese, P.; Bruce, I.; Knapp, M.; Fritsch, C.; Blasco, F.; Blanz, J.; Aichholz, R.; Hamon, J.; Fabbro, D.; Caravatti, G. *Bioorg. Med. Chem. Lett.* **2013**, *23*, 3741.
13. Berg, S.; Bergh, M.; Hellberg, S.; Högdin, K.; Lo-Alfredsson, Y.; Söderman, P.; von Berg, S.; Weigelt, T.; Ormö, M.; Xue, Y.; Tucker, J.; Neelissen, J.; Jerning, E.; Nilsson, Y.; Bhat, R. *J. Med. Chem.* **2012**, *55*, 9107. The following crystal structures of GSK3β were used to dock compounds **1** and **4** (PDB ID codes: 4acd and 4acc).
14. 2-(Dimethylamino)acetyl chloride hydrochloride (77 mg, 0.41 mmol) was added to a stirred solution of **4f** (130 mg, 0.35 mmol) and NEt_3 (0.106 mL, 0.76 mmol) in DMF (3 mL). The resulting solution was stirred at 25 °C for 2 h. The mixture was evaporated, adsorbed on silica gel with a 7 N methanolic solution of ammonia and purified by flash chromatography on silica gel eluting with 1–4% methanolic ammonia (7 N) in dichloromethane. The solvent was evaporated to dryness. The residue was triturated in a mixture of ether and ethyl acetate afford **4** (120 mg, 75%) as a pale yellow foam. ^{1}H NMR (DMSO-d_6) 1.55 (m, 1H), 1.73 (m, 1H), 2.00 (m, 2H), 2.20 (s, 6H), 2.80 (m, 1H), 3.03 (m, 2H), 3.16 (m, 2H), 4.05 (s, 3H), 4.10 (m, 1H), 4.35 (m, 1H), 7.58 (m, 3H), 7.72 (m, 1H), 8.18 (d, 2H), 8.28 (d, 2H), 8.82 (s, 1H); MS-ESI *m/z* 462 [MH^+]; Anal. ($C_{22}H_{27}N_{11}O$·0.8% Et_2O·0.5% EtOAc) C, H, N. Found C, 57.27; H, 5.74; N, 32.76; requires C, 57.30; H, 5.98; N, 32.93.
15. Delouvrié, B.; Germain, H.; Harris, C. S.; Lamorlette, M.; Lebraud, H.; Nguyen, H. T. H.; Noisier, A.; Ouvry, G. *Tetrahedron Lett.* **2012**, *53*, 5380.
16. de Koning, P. D.; McAndrew, D.; Moore, R.; Moses, I. B.; Boyles, D. C.; Kissick, K.; Stanchina, C. L.; Cuthbertson, T.; Kamatani, A.; Rahman, L.; Rodriguez, R.; Urbina, A.; Sandoval, A.; Rose, P. R. *Org. Proc. Res. Dev.* **2011**, *15*, 1018.
17. We were later able to deliver the 4-Bpin 1,2,3-triazole reagent for Suzuki approach via direct borylation, see: Davey, P. R. J.; Delouvrié, B.; Dorison-Duval, D.; Germain, H.; Harris, C. S.; Magnien, F.; Ouvry, G.; Tricotet, T. *Tetrahedron Lett.* **2012**, *53*, 6849.
18. (a) Jutzi, P.; Gilge, U. J. *Organomet. Chem.* **1983**, *246*, 163; (b) Nicolaou, K. C.; Pratt, B. A.; Arseniyadis, S.; Wartmann, M.; O'Brate, A.; Giannakakou, P. *ChemMedChem* **2006**, *1*, 41.
19. Armour, D. R.; Price, D. A.; Stammen, B. L. C.; Wood, A.; Perros, M.; Edwards, M. P. *PCT Int. Appl.* WO2,000,039,125.
20. Strotman, N. A.; Chobanian, H. R.; He, J.; Guo, Y.; Dormer, P. G.; Jones, C. M.; Steves, J. E. *J. Org. Chem.* **2010**, *75*, 1733.
21. The minimised electrostatic potential (V_{Min}) in a lone pair region is a useful predictor of the ability of a heteroatom to act as a hydrogen bond acceptor.[23] Calculation of the V_{Min} value was carried out using the electronic structure modelling program Gaussian 09 following a workflow described by Kenny.[24,25]

The first step in the process involved the energy minimization of input structures; this was done using RHF (Restricted Hartree-Fock) and the 6-31G* basis set (the LANL2DZ basis set was implemented for atoms with atomic number ⩾ Argon). The OEChem Toolkit[26] was used to 'recognize' a molecule from the resulting energy minimized atomic geometry. In the second step, electrostatic potentials were calculated using the B3LYP functional and the 6-31+G** basis set. SMARTS[27] pattern matching was used to identify the aromatic nitrogen and the 2 adjacent atoms; a point 1.2 Å along the defined lone pair axis was used as the starting point for the electrostatic potential minimization. The nearest local minimum in the ESP was identified using the prop = (opt,efg) option in Gaussian 09. Calculated V_{Min} values were previously correlated to experimentally measured hydrogen bond basicity allowing the pK_β value to be calculated using the following equation: $pK_\beta = -59.713 \times (V_{min}/\text{kJ mol}^{-1}) - 3.319$. A pK_β value represents the ability of a heteroatom to form a hydrogen bond, based on a model system in which a complex with a standard hydrogen bond donor (*p*-nitrophenol in 1,1,1-trichoroethane) is formed.[28]

22. It should be noted that compounds **1** and **4** showed some activity against the PI3Kδ isoform (enzyme assays), while they were less active against the PI3Kγ isoform and essentially inactive against m-TOR: for **1**, IC_{50} 0.28 μM, 0.020 μM and 15 μM resp. on PI3Kγ, PI3Kδ and m-TOR; for **4**, IC_{50} 0.65 μM, 0.017 μM and 21 μM resp. on PI3Kγ, PI3Kδ and m-TOR.
23. Kenny, P. W. *J. Chem. Soc., Perkin Trans. 2* **1994**, 199.
24. Kenny, P. W. *J. Chem. Inf. Model.* **2009**, *49*, 1234.
25. Frisch, M. J.; Trucks, G. W.; Schlegel, H. B.; Scuseria, G. E.; Robb, M. A.; Cheeseman, J. R.; Scalmani, G.; Barone, V.; Mennucci, B.; Petersson, G. A.; Nakatsuji, H.; Caricato, M.; Li, X.; Hratchian, H. P.; Izmaylov, A. F.; Bloino, J.; Zheng, G.; Sonnenberg, J. L.; Hada, M.; Ehara, M.; Toyota, K.; Fukuda, R.; Hasegawa, J.; Ishida, M.; Nakajima, T.; Honda, Y.; Kitao, O.; Nakai, H.; Vreven, T., ; Montgomery, J. A., Jr.; Peralta, J. E.; Ogliaro, F.; Bearpark, M.; Heyd, J. J.; Brothers, E.; Kudin, K. N.; Staroverov, V. N.; Kobayashi, R.; Normand, J.; Raghavachari, K.; Rendell, A.; Burant, J. C.; Iyengar, S. S.; Tomasi, J.; Cossi, M.; Rega, N.; Millam, J. M.; Klene, M.; Knox, J. E.; Cross, J. B.; Bakken, V.; Adamo, C.; Jaramillo, J.; Gomperts, R.; Stratmann, R. E.; Yazyev, O.; Austin, A. J.; Cammi, R.; Pomelli, C.; Ochterski, J. W.; Martin, R. L.; Morokuma, K.; Zakrzewski, V. G.; Voth, G. A.; Salvador, P.; Dannenberg, J. J.; Dapprich, S.; Daniels, A. D.; Farkas, Ö.; Foresman, J. B.; Ortiz, J. V.; Cioslowski, J.; Fox, D. J. *Gaussian 09, Revision A.1*; Gaussian: Wallingford CT, 2009.
26. OEChem TK—Programming Library for Chemistry and Cheminformatics. OpenEye Scientific Software, Santa Fe, http://www.eyesopen.com/oechem-tk.
27. SMARTS—A Language for Describing Molecular Patterns. Daylight Chemical Information Systems, Inc., CA, USA, http://www.daylight.com/dayhtml/doc/theory/theory.smarts.html.
28. Abraham, M. H.; Duce, P. P.; Prior, D. V.; Barratt, D. G.; Morris, J. J.; Taylor, P. J. *J. Chem. Soc., Perkin Trans. 2* **1989**, 1355.